Thin Solid Films 737 (2021) 138927

Contents lists available at ScienceDirect

Thin Solid Films

journal homepage: www.elsevier.com/locate/tsf

Efficient prediction of elastic properties of $Ti_{0.5}Al_{0.5}N$ at elevated temperature using machine learning interatomic potential

Ferenc Tasnádi [*,a], Florian Bock [a], Johan Tidholm [a], Alexander V. Shapeev [b], Igor A. Abrikosov [a]

[a] IFM, Linköping University, Linköping, SE-581 83, Sweden
[b] Skolkovo Institute of Science and Technology, Moscow, 121205, Russia

ARTICLE INFO

Keywords:
Machine learning
Interatomic potential
Elastic tensor
Finite temperature
Alloys

ABSTRACT

High-temperature thermal stability, elastic moduli and anisotropy are among the key properties, which are used in selecting materials for cutting and machining applications. The high computational demand of ab initio molecular dynamics (AIMD) simulations in calculating elastic constants of alloys promotes the development of alternative approaches. Machine learning concept grasped as hybride classical molecular dynamics and static first principles calculations have several orders less computational costs. Here we prove the applicability of the concept considering the recently developed moment tensor potentials (MTP), where moment tensors are used as material's descriptors which can be trained to predict the elastic constants of the prototypical hard coating alloy, $Ti_{0.5}Al_{0.5}N$ at 900 K. We demonstrate excellent agreement between classical molecular dynamics simulations with MTPs and AIMD simulations. Moreover, we show that using MTPs one overcomes the inaccuracy issues present in approximate AIMD simulations of elastic constants of alloys.

1. Introduction

Hard ceramic coatings are utilized to extend the wear resistance and lifetime of machining tools in the cutting zone subjected to excessive heat and mechanical load. In general, linear elasticity at operational temperature is essential to determine forces acting on dislocations in materials and understand plastic deformations [1]. It means that the knowledge of elastic constants at elevated temperature supports the design of high-strength, wear resistant industrial materials. On the other hand, phase field simulations have shown the impact of elastic energy on microstructure evolution during spinodal decomposition of alloys [2,3] and Zener's elastic anisotropy has contributed to the understanding of the age hardening in $Ti_{(1-x)}Al_xN$ [4–6].

Accessing properties of hard coatings at operational temperature, which is up to around 900-1000 °C [7,8] for TiN based materials, is a challenging task for computer simulations based on the laws of quantum mechanics. Besides the freedoms of the electronic motions described through density functional theory calculations the atomic vibrations have to be simulated and the corresponding vibrational entropy should be calculated. Sophisticated approaches utilizing ab initio molecular dynamics (AIMD) simulations have recently been introduced to include the contribution of atomic vibrations to the material's free energy at arbitrary temperatures. Self-consistent phonon theory [9,10], stochastic self-consistent harmonic approximation [11] or the temperature dependent effective potential method (TDEP) [12] are among the approaches used to calculate effective harmonic force constants to predict, for example, lattice thermal conductivity in cubic $SrTiO_3$ [13], superconducting critical temperature of hydrogen sulfide [14] or phase stability of CrN [15]. Recently, the phase diagram of $Ti_{(1-x)}Al_xN$ random alloys has been calculated using TDEP [16]. The approach has also been extended to predict the elastic tensor of $Ti_{(1-x)}Al_xN$ random alloys at elevated temperatures [17].

A bottleneck of all these calculations is the high computational demand of the underlying AIMD simulations, especially in case of metallic alloys, where a large supercell model is needed in combination with dense k-point sampling in the Brillouin zone. This issue gets more severe in case of predicting elastic constants because of the need for accurate stresses. Density functional theory calculation with approximate exchange-correlation functional typically results in 10% error in comparison with experiment on absolute values, but it is much more accurate in predicting trends e.g. on the temperature dependences. In accelerating computational schemes one does not want to add other errors on top of the density functional theory and the highly accurate (within 1 GPa) predictions of the temperature dependences of elastic

* Corresponding author.
E-mail address: ferenc.tasnadi@liu.se (F. Tasnádi).

https://doi.org/10.1016/j.tsf.2021.138927
Received 8 April 2021; Received in revised form 9 September 2021; Accepted 9 September 2021
Available online 15 September 2021

constants are realistic. One needs ∼1 meV/atom accuracy in energy differences to predict elastic constants with ∼1 GPa accuracy. To moderate the computational demand, approximate AIMD approaches have been introduced; the quasi-static or volume scaled simulations (VSS) [18] and the symmetry imposed force constants (SIFC) approximation combined with the temperature dependent effective potential (SIFC-T-DEP) approach [17].

An alternative to AIMD is to use classical molecular dynamics simulations in which forces and stresses are computed from an empirical interatomic potential (IP). Since classical molecular dynamics does not account for the electronic degrees of freedom the calculation accuracy depends on the applied IP. The classical embedded atom model [19] and modified embedded atom model interatomic potentials [20] can be fitted to carefully performed ab initio calculations to provide quantitative accuracy, however, their applicability for different properties or various materials, phases or compositions is limited by the prescribed functional form of the IP and by the implemented parameter values.

Learning-on-the-fly strategy [21,22] has been suggested to incorporate static first-principles calculations into classical IP models and achieve molecular dynamics trajectories on a quantum mechanical level of accuracy. However, to succeed one needs not only a flexible and complete many-body functional form of the IP but also an effective machine learning strategy. The recently developed moment tensor potential (MTP) approach [23] uses contracted moment tensors as structural descriptors in generating IPs, called MTPs. Furthermore, an active learning method based on the maxvol algorithm [24] has been suggested to train MTPs on-the-fly [25]. Machine learned MTPs have successfully been utilized, for example, in crystal structure search [26], predicting thermal conductivity of complex compounds [27] or modeling self-diffusion in aluminum [28].

In this study, as proof of concept, we show that MTPs can be trained on AIMD simulation results to obtain highly accurate elastic constants of a prototypical hard coating alloy, $Ti_{0.5}Al_{0.5}N$ at 900 K. We note that an active learning approach of MLIP fitting [26] has been applied to accelerate AIMD simulations for elemental metals [29], and for multi-component alloys [30] reduces the computational effort by two orders of magnitude. A comparison of calculated elastic properties using machine learned MTP with values calculated by highly accurate AIMD, as well as by approximate AIMD-based methods [17,31] shows that with the machine learned MTPs one achieves both, high efficiency and excellent accuracy of the simulated results.

2. Methodology

$Ti_{0.5}Al_{0.5}N$ solid solution has been modeled by a $(4 \times 4 \times 4)$ supercell of the B1 unit cell with totally random arrangement of Ti and Al atoms on the metal sublattice. High accuracy AIMD canonical (NVT) simulations have been performed to characterize the material's properties at four different temperatures from 300 K up to 1500 K. In this study we utilize the results of the simulations performed at 900 K. The calculations of the elastic moduli of $Ti_{0.5}Al_{0.5}N$ have been carried out using finite distortions with the distortion matrix

$$\begin{pmatrix} 1+\eta & \eta/2 & 0 \\ \eta/2 & 1 & 0 \\ 0 & 0 & 1 \end{pmatrix} \quad (1)$$

with $\eta = \pm 0.01, \pm 0.02$ strains applied at the calculated equilibrium lattice parameters. The thermal expansion of $Ti_{0.5}Al_{0.5}N$ was extracted from Ref. [17]. At each η around 15,000 AIMD steps with 0.5 fs time step have been performed. The non-equivalent averaged cubic elastic constants C_{11}, C_{12} and C_{44} have been calculated by performing simulations with three orientation of the coordinate system, (xyz), (yzx) and (zxy). A comprehensive discussion of the AIMD simulations and the derived results is out of the scope of the present study and will be presented elsewhere [32].

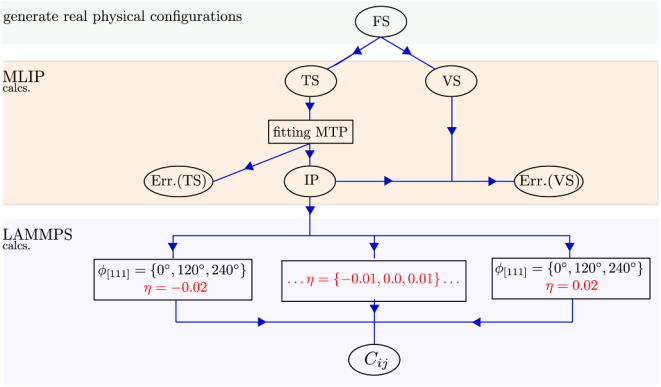

Fig. 1. Flow diagram of the calculation process. See text for the detailed explanation.

Table 1
Total energy errors in eV unit for the fitting Err.(TS) and validation Err.(VS) using a supercell with 128 atoms. The number of parameters in MTP is given in parenthesis, which are optimized using 2000 iterations with energy weight 1.0, force weight 0.01 and stress weight 0.01. TS_1 training sets contain 300 configurations, while TS_2 600 ones. Validation error is checked on 3362 configurations. MAD means maximum absolute difference and RMS stands for root mean square.

model:$MTPTS_x$/Y (# of params.)	Err.(TS)		Err.(VS)	
	MAD	RMS	MAD	RMS
$10gTS_1$/A (232)	0.53217	0.19706	0.58142	0.19011
$10gTS_1$/B (232)	0.64886	0.18602	0.63807	0.21203
$10gTS_1$/C (232)	0.57279	0.19619	0.55249	0.18243
$10gTS_2$/A (232)	0.61891	0.20006	0.61181	0.20546
$10gTS_2$/B (232)	0.62890	0.21274	0.56933	0.22431
$10gTS_2$/C (232)	0.57623	0.20206	0.54565	0.20326
$16gTS_1$/A (380)	0.42558	0.14777	0.48838	0.14882
$16gTS_1$/B (380)	0.48602	0.13407	0.38614	0.13373
$16gTS_1$/C (380)	0.40933	0.14394	0.44103	0.15288
$16gTS_2$/A (380)	0.44770	0.14204	0.51809	0.14837
$16gTS_2$/B (380)	0.43919	0.13893	0.44839	0.14417
$16gTS_2$/C (380)	0.42911	0.14679	0.45565	0.14337
$18gTS_1$/A (523)	0.38434	0.11979	0.39120	0.13629
$18gTS_1$/B (523)	0.37666	0.12785	0.48432	0.13186
$18gTS_1$/C (523)	0.34299	0.12503	0.43094	0.12555
$18gTS_2$/A (523)	0.32090	0.12049	0.34427	0.12597
$18gTS_2$/B (523)	0.38272	0.12420	0.38416	0.12396
$18gTS_2$/C (523)	0.42946	0.13232	0.33737	0.14064
$20gTS_1$/A (648)	0.42169	0.13114	0.33150	0.13066
$20gTS_1$/B (648)	0.36753	0.10710	0.34666	0.12456
$20gTS_1$/C (648)	0.30537	0.10643	0.35318	0.11812
$20gTS_2$/A (648)	0.32904	0.10991	0.40864	0.12878
$20gTS_2$/B (648)	0.37434	0.10661	0.34191	0.11371
$20gTS_2$/C (648)	0.38561	0.10653	0.36188	0.11204
$24gTS_1$/A (1296)	0.29535	0.092023	0.27117	0.10430
$24gTS_1$/B (1296)	0.24038	0.086756	0.28304	0.10210
$24gTS_1$/C (1296)	0.29339	0.089634	0.31206	0.10571
$24gTS_2$/A (1296)	0.30351	0.090331	0.28821	0.10688
$24gTS_2$/B (1296)	0.31187	0.087811	0.30683	0.10080
$24gTS_2$/C (1296)	0.28773	0.088384	0.27129	0.093561

The calculation scheme based on the use of the machine learned MTPs, in general, has three major blocks, as shown in Fig. 1. In the first block an arbitrary method should be utilized to generate a set of atomic arrangements (dataset) at the given thermodynamic conditions with corresponding total energies, stresses and forces (labels) calculated with density functional theory. These labels are used with different weights to fit the MTP. We call this labeled dataset as full set of selected labeled data (FS). In our case, only a selected set of configurations from the above discussed AIMD simulations have been used to create FS. In general, three types of labeled datasets have been created from the total ≈60000 labeled data of the full AIMD simulations: FS, a subset of FS,

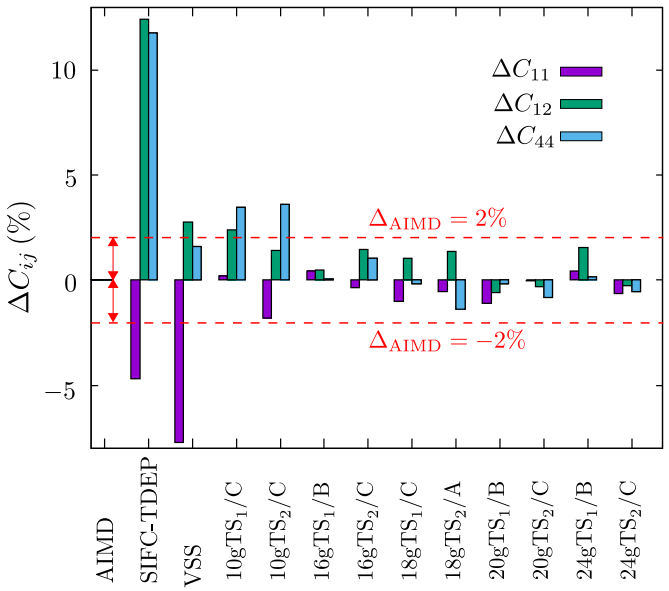

Fig. 2. Relative errors of C_{ij} wrt. AIMD values, C_{11}^{AIMD}=362 GPa, C_{12}^{AIMD}=145 GPa and C_{44}^{AIMD}=187 GPa. See Table 2 for all values.

which is sampled to create training sets (TSs), and a validation set (VS) to validate the trained MTP.

FS has been created as follows. Our aim has been to find a reasonably small but still representative TS, therefore, we have utilized the AIMD simulations performed with ±2% strains only, which have served summing up the three lattice orientations altogether 30000 labeled data. This choice is supported by the argument that TS should provide a representation with sufficient volume variation. The selected six AIMD runs have always been treated independently. We have cut away the first 1000 from each simulations corresponding to the initial equilibration processes. The remaining 24,000 configurations with the corresponding density functional theory calculated total energies, stresses and forces have been combined to define FS.

In the second block of Fig. 1 called MLIP calcs. we have created VS and the training sets (TSs). First a sampling set (SS) has been created by combining the first 2500 configurations from each simulations. To create VS, which is uncorrelated from SS we have skipped 1000 configurations after the selected 2500 configurations and combined the remaining around 500 configurations from the six simulations. Thus, SS has contained around 15,000 configurations while VS around 3000. Training set TS_1 with 300 configurations has been created by randomly selecting 2% of each SS, such that equaly 2% has been selected from each simulations. We have made three independent random sampling resulting in TS_1/A, TS_1/B and $TS1_1$/C. TS_2 training sets have been formed by randomly selecting 4% of each SS. The TS_2 sets have contained 600 at. configurations.

Various levels of approximations have been used in defining the functional form of IP. Depending on the highest degree of polynomial-like basis functions used in the analytic description of the MTP [23], we have used the so called 10g, 16g, 18g, 20g and 24g MTPs. IPs have been derived by fitting the MTPs to TSs using the Broyden-Fletcher-Goldfarb-Shanno method [24] with 2000 iterations and 1.0, 0.01 and 0.01 weights for total energy, stresses and forces in the loss functional.

Elastic constants (C_{ij}) of $Ti_{0.5}Al_{0.5}N$ have been calculated in the third block of Fig. 1 called LAMMPS cals. using averaged stresses and strains extracted from the distortions given by the distortion matrix in Eq. (1) with $\pm 1,2\%$ strain. The elastic tensor has been calculated by employing the symmetrization technique [33] to account for the disorder present in the supercell. This means that we have averaged C_{11}, C_{12} and C_{44} elastic constants calculated with three different orientiations of the same supercell labeled with $\phi_{[111]} = \{0°, 120°, 240°\}$. The classical molecular dynamics simulations with the trained IPs were carried out using the Large-scale Atomic/Molecular Massively Parallel Simulator (LAMMPS) [34] with 1 fs time step and performing 100.000 steps. Note that $Ti_{0.5}Al_{0.5}N$ has been modeled with exactly the same supercell as in the AIMD NVT-simulations.

Table 2
Elastic constanst of $Ti_{0.5}Al_{0.5}N$ at 900 K using TS_1 and TS_2 training sets created from AIMD simulations and fitted to various levels of MTP potentials. The number of parameters in MTPs are given in parenthesis. The supercell size in Lammps calculation is 128 atoms. Sym. stands for symmetry averaged elastic constants. * Ref[17]..

Method / $MTPTS_x$/Y (# of params.)	$\phi_{[111]}$	C_{11} (GPa)	C_{12} (GPa)	C_{44} (GPa)
AIMD		362	146	188
SIFC-TDEP*		379	127	165
VSS*		390	142	184
10gTS_1/C (232)	0°	360	146	180
	120°	360	143	180
	240°	364	136	181
	sym.	361	142	180
10gTS_2/C (232)	0°	365	143	180
	120°	370	142	179
	240°	371	134	181
	sym.	369	143	180
16gTS_1/B (232)	0°	360	142	186
	120°	363	147	187
	240°	358	144	187
	sym.	360	144	187
16gTS_2/C (232)	0°	362	142	185
	120°	366	142	185
	240°	362	145	185
	sym.	363	143	185
18gTS_1/C (232)	0°	366	144	187
	120°	363	149	187
	240°	368	137	187
	sym.	366	143	187
18gTS_2/A (232)	0°	367	141	190
	120°	361	143	190
	240°	364	145	189
	sym.	364	143	190
20gTS_1/B (232)	0°	367	144	188
	120°	365	147	190
	240°	366	146	188
	sym.	366	146	189
20gTS_2/C (232)	0°	361	145	188
	120°	364	148	190
	240°	361	144	188
	sym.	362	145	188
24gTS_1/B (232)	0°	361	147	186
	120°	361	144	188
	240°	360	138	187
	sym.	360	143	187
24gTS_2/C (232)	0°	363	146	187
	120°	362	145	189
	240°	368	145	188
	sym.	364	145	188

3. Results

Table 1 gives an overview of the accuracy of the MTP fitting. By comparing the value of root mean square (RMS) error of the fitting with the validation RMS error one can state that in each cases the choice of TS is representative. Furthermore, the small variation of RMS with changing TS_1/A to B and C rules out overfitting. To predict elastic constants

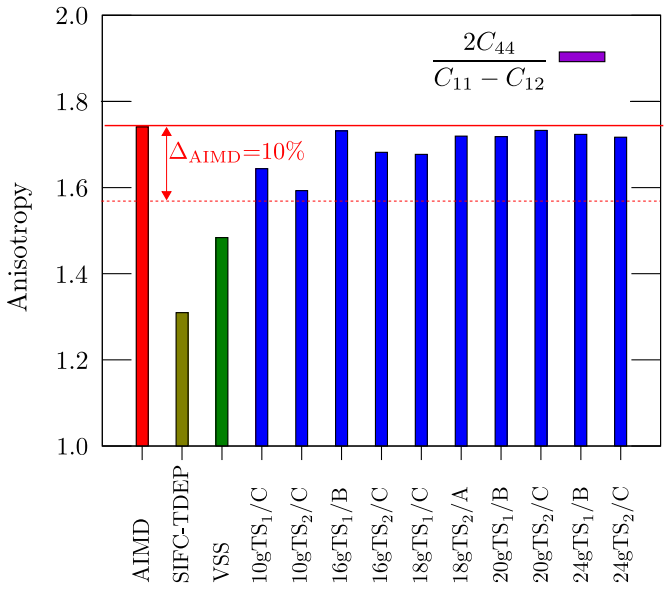

Fig. 3. Zener elastic anisotropy values of $Ti_{0.5}Al_{0.5}N$ calculated by ab initio molecular dynamics (AIMD) simulations without additional approximations, symmetry imposed force constants approximation combined with the temperature dependent effective potential (SIFC-TDEP),the quasi-static or volume scaled simulations (VSS) approximation and different MTPs.

with 1 GPa accuracy one needs 1 meV/atom accuracy in energy differences. Accordingly, with our 128 atoms supercell only 18g, 20g and 24g MTPs fulfill this requirement, see RMS of Err(VS).

In the following we compare elastic constants calculated by different methods. The values are listed in Table 2. C_{11}=362 GPa, C_{12}=145 GPa and C_{44}=187 GPa are the cubic averaged elastic constants obtained by direct highly accurate AIMD simulations [32]. These values are used as reference hereafter. The table also lists the values obtained by applying the SIFC-TDEP[17] and VSS [31] approach.

To calculate elastic constants we have selected the model from Table 1, which results in the smallest RMS error in validation. For example, in the choice of 10g MTP and TS_1 the random selection C, that is the $10gTS_1$/C model results in the smallest RMS. However, in some cases the LAMMPS simulations used to calculate Cij have led to unphysical results for the selected model, e.g. (i) to unphysically large pressure or (ii) to unrealistically large value of the bulk modulus. In such cases we have selected the model with next smallest RMS error in validation, followed by the nex one if the unphysical features remain. For example, in case of 18g and TS_2 the model with second lowest RMS error ($18gTS_2$/A) has resulted in elastic constants. The obtained elastic constants are listed in Table 2.

A comparison of the relative errors of C_{ij}s obtained with different methods is shown in Fig. 2. One sees that from 16g MTPs one obtaines all C_{ij}s with less than 2% error wrt. the highest accurate AIMD values. Zener's type elastic anisotropy values have been calculated and compared in Fig. 3. The range of 10% error from the AIMD calculated value is marked with two dashed lines. One sees that all the MTP potentials result in less than 10% error. However, SIFC-TDEP results in 25% error while VSS in 15%. One sees that from and above the order of 16g MTP the error in predicted Zener's anisotropy is below 4%. The 20g MTP results in less than 1.5% error. In summary, using 20g MTP one achieves an accurate elastic chracterization of $Ti_{0.5}Al_{0.5}N$ at 900 K with less than 2% relative error with respect to highly accurate AIMD simulations.

4. Conclusions

Elastic constats of $Ti_{0.5}Al_{0.5}N$ at 900 K have been calculated using classical molecular dynamics simulations with machine learned moment tensor potentials. Using 16 as the highest degree of polynomial-like basis functions in the analytic description of the moment tensor potential (16g) the accuracy of the predicted elastic constants is within the ± 2% of the values derived from the highly accurate direct ab initio molecular dynamics simulations. In comparison with recently proposed approximate ab initio molecular dynamics based acceleration schemes, which result in 24% error for the Zener elastic anisotropy, 16g moment tensor potentials result in less than 4% difference. Though, in this study the moment tensor potentials have been created using data of ab initio molecular dynamics simulations, we foresee that the potentials can be efficiently trained using an active learning leading to accurate values of elastic constants and greatly improving the efficiency of simulations of mechanical properties of hard coatings at operational conditions of cutting tools.

CRediT authorship contribution statement

Ferenc Tasnádi: Conceptualization, Investigation, Software, Writing – original draft. **Florian Bock:** Investigation, Formal analysis, Writing – review & editing. **Johan Tidholm:** Investigation, Writing – review & editing. **Alexander V. Shapeev:** Conceptualization, Methodology, Software, Writing – review & editing. **Igor A. Abrikosov:** Conceptualization, Formal analysis, Writing – review & editing.

Declaration of Competing Interest

The authors declare the following financial interests/personal relationships which may be considered as potential competing interests:

Ferenc Tasnadi reports financial support was provided by Vinnova Sweden's Innovation Agency. Ferenc Tasnadi reports financial support was provided by Knut and Alice Wallenberg Foundation. Igor A. Abrikosov reports financial support was provided by Swedish Research Council. Ferenc Tasnadi reports a relationship with Swedish Foundation for International Cooperation In Research and Higher Education that includes: travel reimbursement.

Acknowledgements

Support from the Knut and Alice Wallenberg Foundation (Wallenberg Scholar Grant No. KAW-2018.0194), the Swedish Government Strategic Research Areas in Materials Science on Functional Materials at Linköping University (Faculty Grant SFO-Mat-LiU No. 2009 00971) and SeRC, the Swedish Research Council (VR) grant No. 2019–05600 and the VINN Excellence Center Functional Nanoscale Materials (FunMat-2) Grant 2016–05156 is gratefully acknowledged. Development of the MLIP potentials was supported by RFBR grant number 20-53-12012. The computations were enabled by resources provided by the Swedish National Infrastructure for Computing (SNIC) partially funded by the Swedish Research Council through grant agreement no. 2016–07213.

References

[1] D. Hull, J. Bacon D., Introduction to Dislocations, Elsevier, Butterworth-Heinemann, 2011.
[2] D.J. Seol, S.Y. Hu, Y.L. Li, J. Shen, K.H. Oh, L.Q. Chen, Three-dimensional phase-field modeling of spinodal decomposition in constrained films, Met. Mater. Int. 9 (1) (2003) 61–66, https://doi.org/10.1007/BF03027232.
[3] A. Knutsson, I.C. Schramm, K. Asp Grönhagen, F. Mücklich, M. Odén, Surface directed spinodal decomposition at TiAlN/TiN interfaces, J Appl Phys 113 (11) (2013) 114305, https://doi.org/10.1063/1.4795155.
[4] A. Hörling, L. Hultman, M. Odén, J. Sjölén, L. Karlsson, Thermal stability of arc evaporated high aluminum-content $Ti_{(1-x)}Al_xN$ thin films, Journal of Vacuum Science & Technology A 20 (5) (2002) 1815–1823, https://doi.org/10.1116/1.1503784.
[5] P.H. Mayrhofer, A. Hörling, L. Karlsson, J. Sjölén, T. Larsson, C. Mitterer, L. Hultman, Self-organized nanostructures in the ti-al-n system, Appl Phys Lett 83 (10) (2003) 2049–2051, https://doi.org/10.1063/1.1608464.

[6] F. Tasnádi, I.A. Abrikosov, L. Rogström, J. Almer, M.P. Johansson, M. Odén, Significant elastic anisotropy in $Ti_{1-x}Al_xN$ alloys, Appl. Phys. Lett. 97 (23) (2010) 231902, https://doi.org/10.1063/1.3524502.
[7] M. Bartosik, C. Rumeau, R. Hahn, Z.L. Zhang, P.H. Mayrhofer, Fracture toughness and structural evolution in the tialn system upon annealing, Sci Rep 7 (1) (2017) 1–9, https://doi.org/10.1038/s41598-017-16751-1.
[8] N. Norrby, M.P. Johansson, R. M'Saoubi, M. Odén, Pressure and temperature effects on the decomposition of arc evaporated $Ti_{0.6}Al_{0.4}N$ coatings in continuous turning, Surf. Coat. Technol. 209 (2012) 203–207.
[9] N.R. Werthamer, Self-consistent phonon formulation of anharmonic lattice dynamics, Phys. Rev. B 1 (2) (1970) 572–581, https://doi.org/10.1103/PhysRevB.1.572.
[10] T. Tadano, S. Tsuneyuki, First-principles lattice dynamics method for strongly anharmonic crystals, J. Phys. Soc. Jpn. 87 (4) (2018) 041015.
[11] I. Errea, M. Calandra, F. Mauri, Anharmonic free energies and phonon dispersions from the stochastic self-consistent harmonic approximation: application to platinum and palladium hydrides, Phys. Rev. B 89 (6) (2014) 064302, https://doi.org/10.1103/PhysRevB.89.064302.
[12] O. Hellman, P. Steneteg, I.A. Abrikosov, S.I. Simak, Temperature dependent effective potential method for accurate free energy calculations of solids, Phys. Rev. B 87 (10) (2013) 104111, https://doi.org/10.1103/PhysRevB.87.104111.
[13] T. Tadano, S. Tsuneyuki, Self-consistent phonon calculations of lattice dynamical properties in cubic $srtio_3$ with first-principles anharmonic force constants, Phys. Rev. B 92 (5) (2015) 054301, https://doi.org/10.1103/PhysRevB.92.054301.
[14] I. Errea, M. Calandra, C.J. Pickard, J. Nelson, R.J. Needs, Y. Li, H. Liu, Y. Zhang, Y. Ma, F. Mauri, High-pressure hydrogen sulfide from first principles: a strongly anharmonic phonon-mediated superconductor, Phys. Rev. Lett. 114 (15) (2015) 157004, https://doi.org/10.1103/PhysRevLett.114.157004.
[15] N. Shulumba, B. Alling, O. Hellman, E. Mozafari, P. Steneteg, M. Odén, I. A. Abrikosov, Vibrational free energy and phase stability of paramagnetic and antiferromagnetic crn from ab initio molecular dynamics, Phys. Rev. B 89 (17) (2014) 174108, https://doi.org/10.1103/PhysRevB.89.174108.
[16] N. Shulumba, O. Hellman, Z. Raza, B. Alling, J. Barrirero, F. Mücklich, I. A. Abrikosov, M. Odén, Lattice vibrations change the solid solubility of an alloy at high temperatures, Phys. Rev. Lett. 117 (20) (2016) 205502.
[17] N. Shulumba, O. Hellman, L. Rogström, Z. Raza, F. Tasnádi, I.A. Abrikosov, M. Odén, Temperature-dependent elastic properties of tialn alloys, Appl. Phys. Lett. 107 (23) (2015) 231901, https://doi.org/10.1063/1.4936896.
[18] Y. Wang, J.J. Wang, H. Zhang, V.R. Manga, S.L. Shang, L.-Q. Chen, Z.-K. Liu, A first-principles approach to finite temperature elastic constants, J. Phys.: Condens. Matter 22 (22) (2010) 225404.
[19] M.S. Daw, M.I. Baskes, Semiempirical, quantum mechanical calculation of hydrogen embrittlement in metals, Phys. Rev. Lett. 50 (17) (1983) 1285–1288, https://doi.org/10.1103/PhysRevLett.50.1285.
[20] M.I. Baskes, J.S. Nelson, A.F. Wright, Semiempirical modified embedded-atom potentials for silicon and germanium, Phys. Rev. B 40 (9) (1989) 6085–6100, https://doi.org/10.1103/PhysRevB.40.6085.
[21] G. Csányi, T. Albaret, M.C. Payne, A. De Vita, "Learn on the fly": a hybrid classical and quantum-mechanical molecular dynamics simulation, Phys. Rev. Lett. 93 (17) (2004) 175503, https://doi.org/10.1103/PhysRevLett.93.175503.
[22] R. Jinnouchi, F. Karsai, G. Kresse, On-the-fly machine learning force field generation: application to melting points, Phys. Rev. B 100 (1) (2019) 014105, https://doi.org/10.1103/PhysRevB.100.014105.
[23] A.V. Shapeev, Moment tensor potentials: a class of systematically improvable interatomic potentials, Multiscale Model. Simul. 14 (3) (2016) 1153–1173, https://doi.org/10.1137/15M1054183.
[24] R. Fletcher, Practical Methods of Optimization, 2nd ed, Wiley, Chichester ; New York, 1987.
[25] E.V. Podryabinkin, A.V. Shapeev, Active learning of linearly parametrized interatomic potentials, Comput. Mater. Sci 140 (2017) 171–180, https://doi.org/10.1016/j.commatsci.2017.08.031.
[26] E.V. Podryabinkin, E.V. Tikhonov, A.V. Shapeev, A.R. Oganov, Accelerating crystal structure prediction by machine-learning interatomic potentials with active learning, Phys. Rev. B 99 (6) (2019) 064114, https://doi.org/10.1103/PhysRevB.99.064114.
[27] P. Korotaev, I. Novoselov, A. Yanilkin, A. Shapeev, Accessing thermal conductivity of complex compounds by machine learning interatomic potentials, Phys. Rev. B 100 (14) (2019) 144308, https://doi.org/10.1103/PhysRevB.100.144308.
[28] I.I. Novoselov, A.V. Yanilkin, A.V. Shapeev, E.V. Podryabinkin, Moment tensor potentials as a promising tool to study diffusion processes, Comput. Mater. Sci 164 (2019) 46–56, https://doi.org/10.1016/j.commatsci.2019.03.049.
[29] A.V. Shapeev, E.V. Podryabinkin, K. Gubaev, F. Tasnádi, I.A. Abrikosov, Elinvar effect in *beta*-Ti simulated by on-the-fly trained moment tensor potential, New J. Phys. 22 (2020) 113005.
[30] K. Gubaev, Y. Ikeda, F. Tasnádi, J. Neugebauer, A.V. Shapeev, B. Grabowski, F. Körmann, Finite-temperature interplay of structural stability, chemical complexity, and elastic properties of bcc multicomponent alloys from ab initio trained machine-learning potentials, Phys. Rev. Mater. 5 (2021) 073801, https://doi.org/10.1103/PhysRevMaterials.5.073801.
[31] S.-L. Shang, H. Zhang, Y. Wang, Z.-K. Liu, Temperature-dependent elastic stiffness constants of α- and θ-Al2o3from first-principles calculations, J. Phys.: Condens. Matter 22 (37) (2010) 375403.
[32] J. Tidholm, F. Tasnádi, I. Abrikosov, accepted for publications in Thin Solid Films (2021).
[33] F. Tasnádi, M. Odén, I.A. Abrikosov, Ab initio elastic tensor of cubic $Ti_{0.5}Al_{0.5}N$ alloys: dependence of elastic constants on size and shape of the supercell model and their convergence, Phys. Rev. B 85 (14) (2012) 144112, https://doi.org/10.1103/PhysRevB.85.144112.
[34] S. Plimpton, Fast parallel algorithms for short-range molecular dynamics, J. Comput. Phys. 117 (1) (1995) 1–19, https://doi.org/10.1006/jcph.1995.1039.